Non-Markovian dynamics of quantum systems. II. Decay rate, capture, and pure states

Yu. V. Palchikov,[1] Z. Kanokov,[1,2] G. G. Adamian,[1,3] N. V. Antonenko,[1] and W. Scheid[4]
[1]*Joint Institute for Nuclear Research, 141980 Dubna, Russia*
[2]*National University, 700174 Tashkent, Uzbekistan*
[3]*Institute of Nuclear Physics, 702132 Tashkent, Uzbekistan*
[4]*Institut für Theoretische Physik der Justus-Liebig-Universität, D-35392 Giessen, Germany*
(Received 8 June 2004; published 18 January 2005)

On the basis of a master equation for the reduced density matrix of open quantum systems, we study the influence of time-dependent friction and diffusion coefficients on the decay rate from a potential well and the capture probability into a potential well. Taking into account the mixed diffusion coefficient D_{qp}, the quasistationary decay rates are compared with the analytically derived Kramers-type formulas for different temperatures and frictions. The diffusion coefficients supplying the purity of states are derived for a non-Markovian dynamics.

DOI: 10.1103/PhysRevE.71.016122 PACS number(s): 05.30.−d, 03.65.−w, 24.60.−k

I. INTRODUCTION

This paper is the continuation of the first paper (paper I) where we developed the formalism [1]. Here we apply the theoretical results to decay rates, capture, and pure states.

In order to describe the evolution of a quantum system in some relevant collective coordinate q which is coupled with many other degrees of freedom (environment), one needs stohastic forces and a density matrix formalism. As was found in Refs. [2–14], the dynamics of the quantum system in the presence of dissipation and diffusion strongly depends on the coupling with the environment. The Hamiltonian H of the total system can be written

$$H = H_c + H_b + H_{cb}, \tag{1}$$

where $H_c = p^2/(2\mu) + U(q)$ is related to the relevant subsystem with the coordinate q and momentum p, H_b describes the environment, and H_{cb} describes the coupling between these two systems. If we assume an environment consisting of a large set of harmonic oscillators and if H_c is linear in q, the method developed in Ref. [1] yields the friction and diffusion coefficients $\lambda_p(t) \geqslant 0$, $\lambda_q(t) \equiv 0$ and $D_{pp}(t) > 0$, $D_{qp}(t)$, $D_{qq}(t) \equiv 0$, respectively.

The reduced density matrix ρ [15–21] obeys the following equation:

$$\begin{aligned}\frac{d\rho}{dt} = &-\frac{i}{\hbar}[\tilde{H}_c, \rho] - \frac{i}{2\hbar}\lambda_p(t)[q, (\rho p + p\rho)] \\ &+ \frac{i}{2\hbar}\lambda_q(t)[p, (\rho q + q\rho)] - \frac{1}{\hbar^2}D_{pp}(t)[q, [q, \rho]] \\ &- \frac{1}{\hbar^2}D_{qq}(t)[p, [p, \rho]] \\ &+ \frac{1}{\hbar^2}D_{qp}(t)([p, [q, \rho]] + [q, [p, \rho]]),\end{aligned} \tag{2}$$

where $\tilde{H}_c = p^2/(2\mu) + \tilde{U}(q)$ is renormalized collective Hamiltonian. Since in Ref. [1] the friction and diffusion coefficients were self-consistently calculated, this set of coefficients should secure the non-negativity of the density matrix at any time. This holds true for the case $D_{qq}(t) = 0$. This occurs in spite of the violation of the constraint for time-independent diffusion and friction constants [17–21],

$$D_{pp}D_{qq} - D_{qp}^2 \geqslant \frac{\hbar^2(\lambda_p + \lambda_q)^2}{16}, \tag{3}$$

which is at any time a sufficient condition for time-independent diffusion and friction coefficients in order that the uncertainty inequality holds:

$$\sigma = \sigma_{pp}\sigma_{qq} - \sigma_{pq}^2 \geqslant \frac{\hbar^2}{4}.$$

Here, $\sigma_{pp} = \mathrm{Tr}[(p-\overline{p})^2\rho]$, $\sigma_{qq} = \mathrm{Tr}[(q-\overline{q})^2\rho]$, $\sigma_{qp} = 0.5\,\mathrm{Tr}\{[(p-\overline{p})(q-\overline{q}) + (q-\overline{q})(p-\overline{p})]\rho\}$, $\overline{p} = \mathrm{Tr}(p\rho)$, and $\overline{q} = \mathrm{Tr}(q\rho)$. If the coupling H_{cb} with the environment is proportional to p as well as q, then all friction and diffusion coefficients in Eq. (2) are different from zero [1] and satisfy the constraint (3).

In the present paper we study the influence of the time dependence of the friction and diffusion coefficients derived in Ref. [1], with H_{cb} proportional only to q [fully coupled (FC) oscillator], on the results obtained with Eq. (2). The role of the nondiagonal diffusion coefficient D_{qp} is especially investigated. As an example, we calculate the flow rate through a potential barrier in an anharmonic potential with these transport coefficients. The calculated results are compared with the ones obtained with the analytical expressions derived in Ref. [13] for the probability rate through a barrier as well as with the results obtained with a "classic" set of diffusion coefficients.

The master equation (2) describes the dissipative quantum dynamics approximately for anharmonic systems. However, in our case we consider only the initial stage (short time) of the evolution of a system up to the moment when the flow rate reaches the quasistationary regime. For example, in the case of the decay process the system wave function is localized mainly in the initial pocket which can be nicely approximated by a harmonic oscillator. So we can suppose that the influence of higher-order fluctuations on the evolution of systems in the considered stage of the processes is small. If the distribution function spreads out a more complicated poten-

 ©2005 The American Physical Society

tial, its long-time behavior is defined by the general master equation with coordinate- and time-dependent transport coefficients. Without a coordinate dependence of the transport coefficients the regime of weak dissipation and high temperature is suitable for anharmonic systems.

II. TIME-DEPENDENT FRICTION AND DIFFUSION COEFFICIENTS

The expressions for the FC oscillator obtained in Ref. [1] for the friction and diffusion coefficients contain three parameters ω, λ, and γ. The value of γ, which characterizes the width of the environment states, should satisfy the condition $\gamma \gg \omega$. We set $\hbar\gamma = 12$ MeV in our calculations. Here, ω is the frequency of the oscillator which after renormalization $\omega \to \tilde{\omega}$ approximates the potential around the minimum. Due to the interaction with the environment, the potential $U(q)$ is renormalized because there is no compensating term in Eq. (1) as in Ref. [8]. In the applications in which we are interested, this renormalization leads to a weak dependence of the frequency $\omega(t)$ on time until it reaches the asymptotic value $\tilde{\omega}$. The values of parameters λ and ω are set so as to obtain a given asymptotics $\tilde{\omega} = \omega(\infty)$ and $\lambda_p = \lambda_p(\infty)$ at fixed temperature T. For $\mu = 50 m_0$ (m_0 is the mass of nucleon) and $\hbar\tilde{\omega} = 3$ MeV, the time dependence of the friction and diffusion coefficients is presented in Fig. 1 at the initial conditions $\lambda_p(t=0) = 0$, $D_{pp}(t=0) = 0$, and $D_{qp}(t=0) = 0$. After some transient time τ the coefficients reach their asymptotic values $\lambda_p(\infty)$, $D_{pp}(\infty)$, and $D_{qp}(\infty)$. While λ_p and D_{pp} are positive at any time, D_{qp} is positive during a short initial time and becomes negative for large times. The transient time is quite short: $\tau \ll 2\pi/\tilde{\omega}$. As follows from the analytical expressions [1], $D_{pp}(\infty)$ is proportional to $\lambda_p(\infty)$ and the value of $D_{qp}(\infty)$ decreases with increasing $\lambda_p(\infty)$ and increases with T.

The asymptotic value $D_{pp}(\infty)$ obtained in Ref. [22] is almost the same as the value of D_{pp} in Ref. [1] and here. Due to the simplifications made in Ref. [22], the value of $D_{qp} < 0$ obtained there is about 25% smaller than our value of $D_{qp}(\infty)$.

Since the friction and diffusion coefficients were derived with a linear coupling in the coordinate between the collective subsystem and environment, we have $D_{qq} = 0$ and $\lambda_p = 0$ at any time. In the present paper we restrict ourselves to this coupling and use three sets of friction and diffusion coefficients in the numerical examples. The first set is the time-dependent set of the coefficients derived in the part I [see Eqs. (33)–(35), (57), and (58) in Ref. [1]] and shown for $\lambda_p(\infty) = 1$ MeV and $T = 0.1$ MeV in Fig. 1:

$$\text{(i)} \quad D_{pp}(t), \quad D_{qp}(t), \quad \lambda_p(t). \tag{4}$$

The second set contains the asymptotic values of these coefficients [see Eqs. (59) and (60) in Ref. [1]]:

$$\text{(ii)} \quad D_{pp}(\infty), \quad D_{qp}(\infty), \quad \lambda_p(\infty). \tag{5}$$

Comparing the results obtained with Eqs. (4) and (5), one can elucidate the role of the dependence of the friction and diffusion on time. The third set of coefficients coincides with the first set but the coefficient D_{qp} is assumed to be zero:

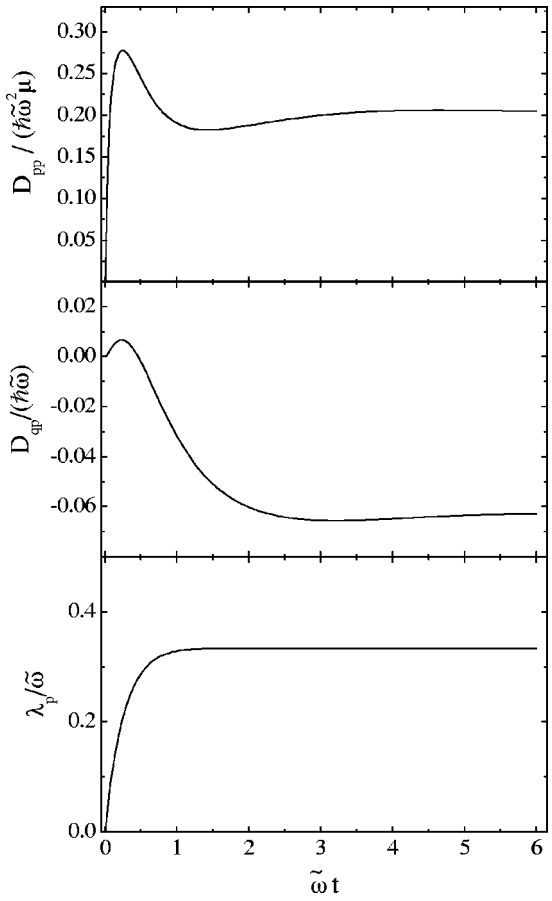

FIG. 1. Time dependent diffusion coefficients $D_{pp}(t)$ and $D_{qp}(t)$ and friction coefficients $\lambda_p(t)/\tilde{\omega} \to 0.33$ calculated for $\hbar\tilde{\omega} = 3$ MeV, $\mu = 50 m_0$, and $T/(\hbar\tilde{\omega}) = 0.033$.

$$\text{(iii)} \quad D_{pp}(t), \quad D_{qp}(t) \equiv 0, \quad \lambda_p(t). \tag{6}$$

Comparing the results obtained with Eqs. (4) and (6), one can conclude on the role of D_{qp} in the evolution of the system. The results obtained with these sets of friction and dif-

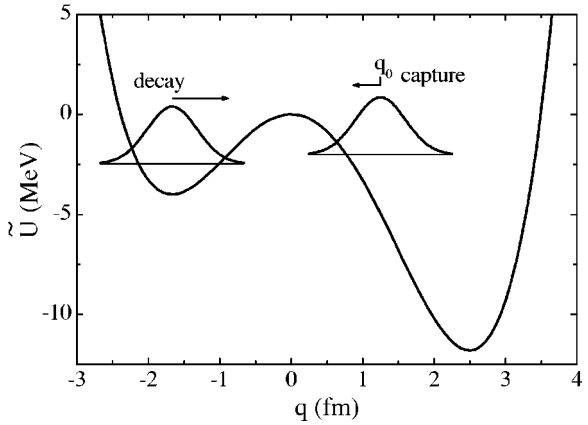

FIG. 2. Bistable potential (8). The schematically shown Gaussian packet in the left well decays into the right-hand potential well. The left-hand packet approaching the barrier from the right-hand side is partly captured.

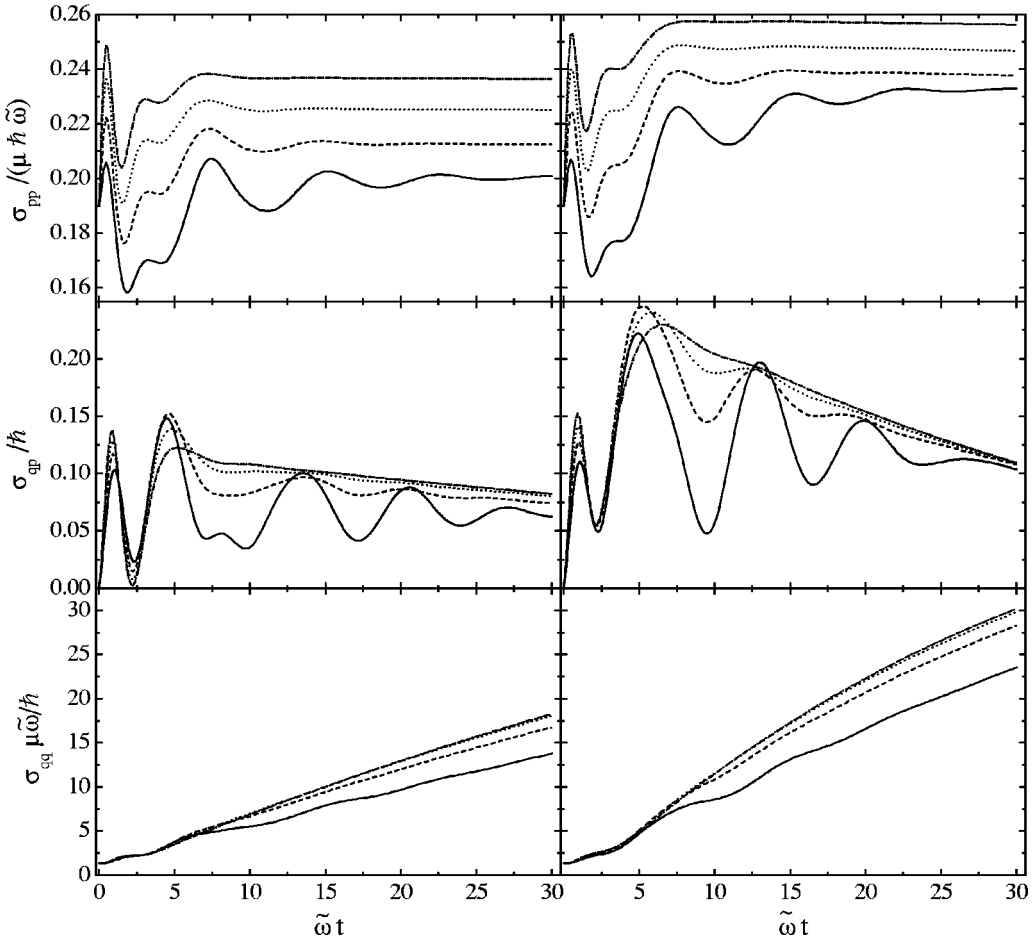

FIG. 3. Time dependence of the variances $\sigma_{pp}(t)$, $\sigma_{qp}(t)$, and $\sigma_{qq}(t)$ for the decay of the initially Gaussian packet from the left-hand well of the potential (8) at $\mu=50m_0$ and $\hbar\tilde{\omega}=3$ MeV for the temperatures $T/(\hbar\tilde{\omega})=0.033$ (left side) and 0.33 (right side) and friction coefficients $\lambda_p/\tilde{\omega}=0.17$ (solid lines), 0.33 (dashed lines), 0.50 (dotted lines), and 0.66 (dash-dotted lines).

fusion coefficients can be compared with the widely used classic diffusion coefficients

$$\text{(iv)} \quad D_{pp}^{c}=\mu\lambda_p T^*, \quad D_{qq}=D_{qp}=0, \tag{7}$$

where the effective temperature is $T^*=0.5\hbar\tilde{\omega}\coth[\hbar\tilde{\omega}/(2T)]$.

III. DECAY RATE FROM THE POTENTIAL WELL

A. Asymmetric bistable potential

Let us study the escape of a Gaussian packet from a shallow well to a deeper well of an asymmetric bistable potential (Fig. 2) presented by a polynom of the fourth order:

$$\tilde{U}(q)=-\frac{6q_R V_L}{q_L^2(2q_R-q_L)}q^2-\frac{4(q_L+q_R)V_L}{q_L^3(q_L-2q_R)}q^3-\frac{3V_L}{q_L^3(2q_R-q_L)}q^4, \tag{8}$$

where q_L and q_R are the positions of the left and right minima, respectively, and V_L is the depth of the left minima. Note that the barrier is at $q=q_b=0$. For the calculations, we set $V_L=4$ MeV, $q_L=-1.67$ fm, and $q_R=2.5$ fm. With these parameters the depth of the right well is 11.8 MeV. We consider two values of the mass parameter μ, $50m_0$ and $448m_0$, corresponding to the frequency at the left potential minima, $\hbar\tilde{\omega}_m=3$ MeV and $\hbar\tilde{\omega}_m=1$ MeV, respectively. The initial Gaussian distribution is centered at q_L and has the square root of the variance $\sqrt{\sigma_{qq}(0)}=0.35$ fm and $\sqrt{\sigma_{qq}(0)}=0.2$ fm for $\mu=50m_0$ and $448m_0$, respectively. The variances $\sigma_{pp}(0)$ are chosen from the uncertainty relation with $\sigma_{qp}=0$: $\sigma_{pp}(0)=\hbar^2/[4\sigma_{qq}(0)]$.

The calculated time-dependent variances $\sigma_{pp}(t)$, $\sigma_{qp}(t)$, and $\sigma_{qq}(t)$ are presented in Figs. 3 and 4 for the different mass values. For $t>4\hbar/\text{MeV}$, $\sigma_{pp}(t)$ reaches the asymptotic value, when the equilibrium in momentum is established in the bistable-type potential. With smaller mass and friction the quantities $\sigma_{pp}(t)$ and $\sigma_{qp}(t)$ have more oscillations in time. For a larger mass, the relative increase of the values of variances with temperature is larger. At large time the value of $\sigma_{qp}(t)$ changes slowly. Since the initial Gaussian state is destroyed because of the escape of the packet into the right well (see Fig. 2), the value of $\sigma_{qq}(t)$ increases with time in the considered time interval. While the values of $\sigma_{qq}(t)$ and $\sigma_{qp}(t)$ increase with λ_p for smaller mass, they decrease with increasing λ_p for larger mass. This occurs due to the balance between the diffusion and friction. For small mass, the diffusion can overcompensate the decrease of the escape rate

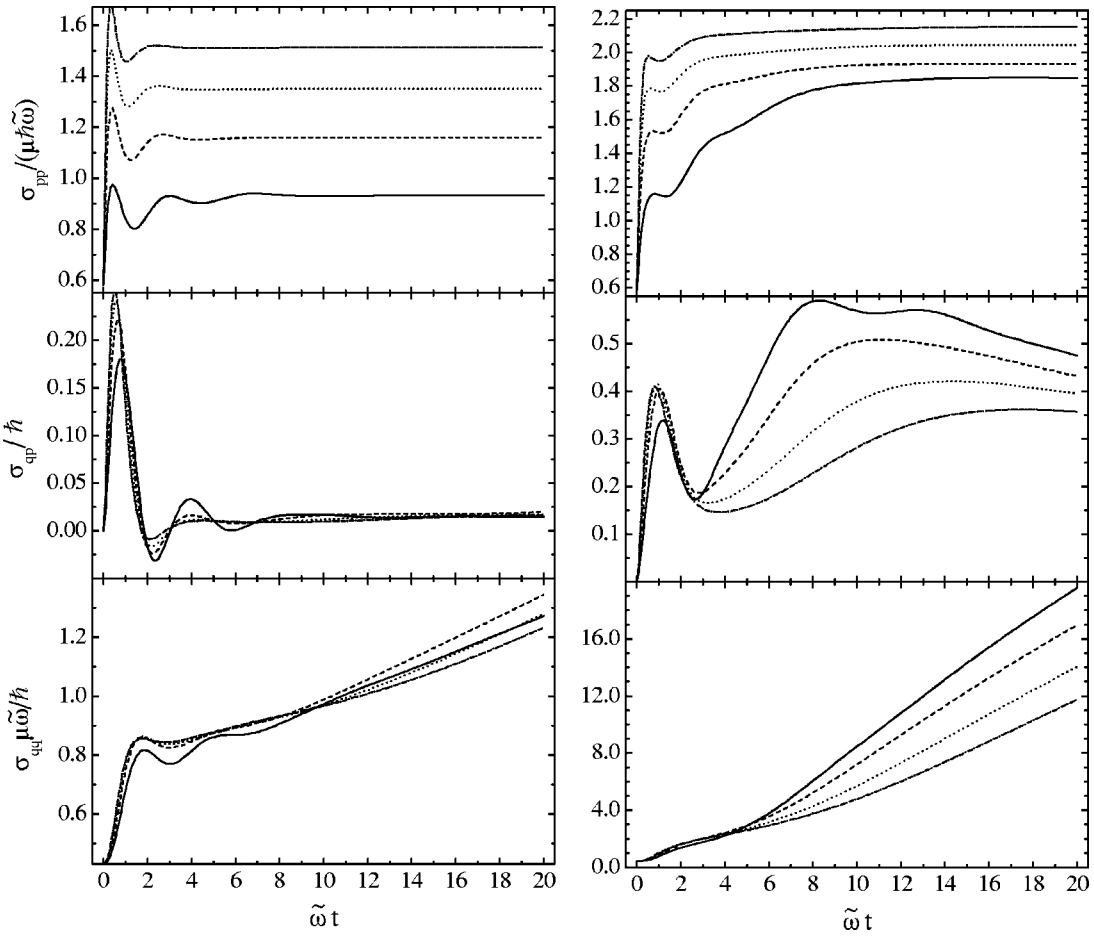

FIG. 4. Time dependence of the variances $\sigma_{pp}(t)$, $\sigma_{qp}(t)$, and $\sigma_{qq}(t)$ for the decay of the initially Gaussian packet from the left-hand well of the potential (8) at $\mu=448m_0$ and $\hbar\tilde{\omega}=1$ MeV for the temperatures $T/(\hbar\tilde{\omega})=0.5$ (left side) and 1.5 (right side) and friction coefficients $\lambda_p/\tilde{\omega}=0.5$ (solid lines), 1.0 (dashed lines), 1.5 (dotted lines), and 2.0 (dash-dotted lines).

due to the friction. With the second set (5) of friction and diffusion coefficients the time dependence of the variances seems to be similar, especially at large time. Therefore, in many applications one can disregard the time dependence of the friction and diffusion coefficients and use the asymptotic values of λ_p, D_{pp}, and D_{qp}.

In spite of the violation of inequality (3) the use of the friction and diffusion coefficients (4) does not lead to a violation of the uncertainty relation due to the about 1.5 times larger coefficient D_{pp} in comparison to the classic value of D_{pp}^c in Eq. (7). With the diffusion coefficients (7) one can observe a violation of the uncertainty relation at the initial time (Fig. 5).

B. Definition of decay rate

Solving the master equation (2) with the above mentioned sets of friction and diffusion coefficients, one can obtain the time-dependent density matrix $\rho(q,t)=\langle q|\hat{\rho}(t)|q\rangle$ in coordinate representation and find the probability $P(t)$ of penetrability of a particle with mass μ through a barrier which has its top at $q=q_b$:

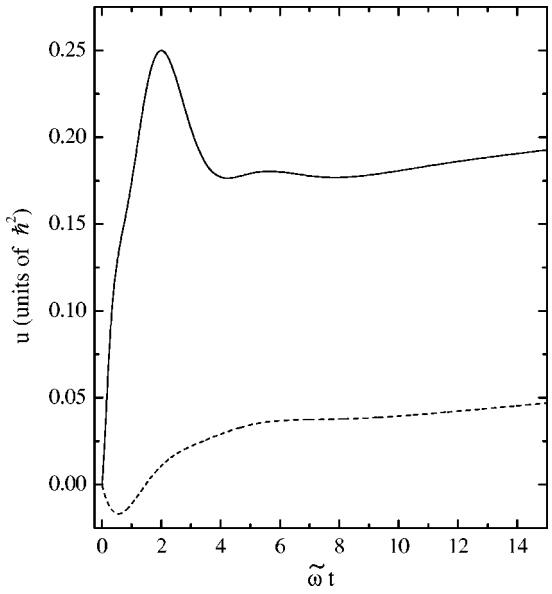

FIG. 5. Time dependence of the uncertainty relation $u(t)=\sigma_{pp}(t)\sigma_{qq}(t)-\sigma_{qp}^2(t)-\hbar^2/4$ at the beginning of the decay process from the left well of the potential (8) with diffusion coefficients (4) (solid line) and (7) (dashed line). The calculations are performed with $\mu=448m_0$, $\hbar\tilde{\omega}=1$ MeV, $\lambda_p/\tilde{\omega}=1$, and $T/(\hbar\tilde{\omega})=0.1$.

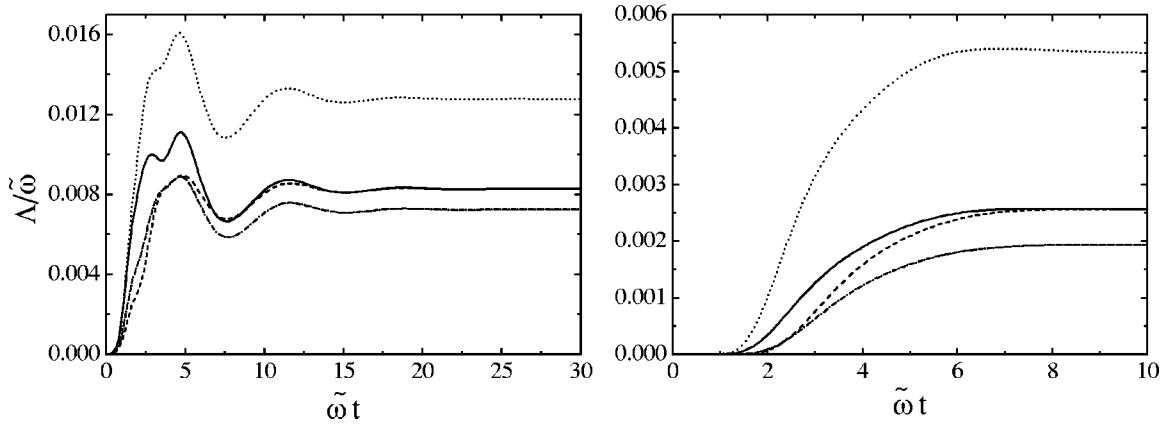

FIG. 6. Time dependences of the decay rate $\Lambda(t)/\tilde{\omega}$ from the left well in the potential (8) at $\mu=50m_0$ (left-hand side), $\mu=448m_0$ (right-hand side), $\lambda_p/\tilde{\omega}=1/(\hbar\tilde{\omega})$, and $T/(\hbar\tilde{\omega})=1/(\hbar\tilde{\omega})$. The results obtained with the time-dependent diffusion coefficients (4), their asymptotic values (5) and the diffusion coefficients (6) are presented by solid, dashed, and dotted lines, respectively. The results obtained with the "classic" diffusion coefficients (7) are presented by dash-dotted lines.

$$P(t)=\int_{q_b}^{\infty}dq[\rho(q,t)-\rho(q,t=0)]\Big/\int_{-\infty}^{q_b}dq\,\rho(q,0), \quad (9)$$

as well as a time-dependent value of the probability rate

$$\Lambda(t)=\frac{1}{1-P(t)}\frac{dP(t)}{dt}. \quad (10)$$

Equation (2) is solved as described in Refs. [11,12] by using an oscillator basis. This method allows us to obtain a solution for ρ from Eq. (2) for any continuous potential and any set of friction and diffusion coefficients.

C. Illustrative calculations

The time dependence of the probability rate $\Lambda(t)$ with respect to $\tilde{\omega}$ over the barrier in the potential (8) for the three sets (4)–(6) of the friction and diffusion coefficients are shown in Fig. 6 for $\hbar\lambda_p=1$ MeV and $T=1$ MeV for two different masses. One can see a minor influence of the time dependence of the friction and diffusion at large t. The sets (4) and (5) lead to the same stationary value of the probability rate $\Lambda(t)$. For small times, $\Lambda(t)$ is larger with the time-dependent set because $D_{pp}(t)$ initially increases and exceeds its asymptotic value. The probability rate $\Lambda(t)$ has more oscillations in time for a smaller (larger) mass (frequency $\tilde{\omega}$)—i.e., when the system approaches to the underdamped regime. The classic set (7) of diffusion coefficients leads to slightly smaller asymptotic values of Λ. The similarity of the asymptotic Λ obtained with the diffusion coefficients (4), (5), and (7) confirms the applicability of the classic set of diffusion coefficients to the problems of the barrier penetrability in the case of a linear coupling in q with the environment.

With the set (6) of diffusion coefficients the probability rate is larger in Fig. 6 than for the set (4) since the negative value of D_{qp} of set (4) keeps the rate $\Lambda(t)$ smaller. In order to obtain the same rate for the case of $D_{qp}=0$, we should decrease the diffusion coefficient D_{pp} by a factor of $\kappa<1$ and use $D'_{pp}=\kappa D_{pp}$ in (6) instead of D_{pp}. The dependence of κ on λ_p is presented in Fig. 7. For $\hbar\lambda_p>1.5$ MeV, κ weakly depends on λ_p and is sensitive to the temperature.

The time dependence of $\Lambda(t)$ is presented for different frictions and temperatures in Fig. 8. The value of $\Lambda(t)$ increases with T. For smaller friction and mass, $\Lambda(t)$ is a more oscillating function of t. While for a large frequency $\tilde{\omega}$ (small μ) the stationary probability rate can increase with λ_p, it decreases for a small frequency $\tilde{\omega}$ (large μ) and large T with increasing λ_p within the considered interval of λ_p. This result for Λ is in agreement with the result of Ref. [13] and is explained by the larger role of prohibiting diffusion in comparison to the minor role of suppressing friction. The dependence of the quasistationary Λ on T and λ_p is presented in Fig. 9 for two values of $\tilde{\omega}$. When the system is near to the underdamped regime, the quasistationary probability rate increases with λ_p within a large interval of λ_p. However, the further increase of λ_p finally leads to a smaller Λ. In the overdamped regime the quasistationary probability rate always decreases with increasing λ_p.

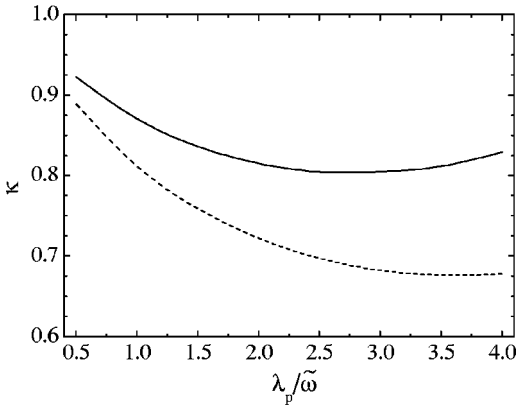

FIG. 7. Dependence of the factor κ on $\lambda_p/\tilde{\omega}$, for $T/(\hbar\tilde{\omega})=1.0$ (solid line) and 0.1 (dashed line).

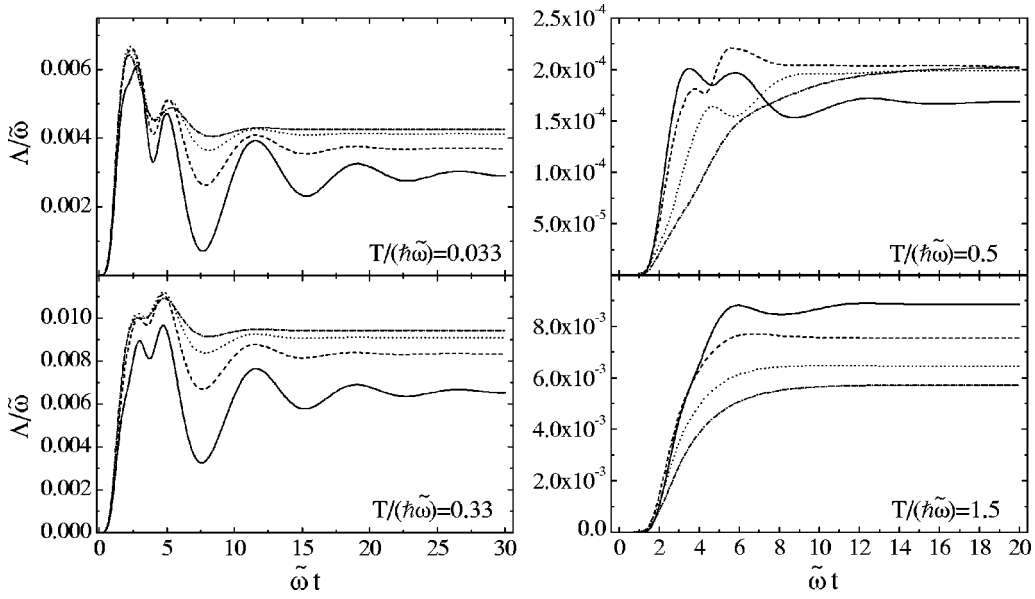

FIG. 8. Time dependence of decay rate $\Lambda(t)/\tilde{\omega}$ from the left well in the potential (8) for $\mu=50m_0$ (left side) and $\mu=448m_0$ (right side) and the indicated temperatures. In the calculations the diffusion coefficients (4) are used with the friction coefficients $\lambda_p/\tilde{\omega}=0.5/(\hbar\tilde{\omega})$ (solid lines), $1.0/(\hbar\tilde{\omega})$ (dashed lines), $1.5/(\hbar\tilde{\omega})$ (dotted lines), and $2.0/(\hbar\tilde{\omega})$ (dash-dotted lines).

D. Comparison with Kramers-type expressions

In Ref. [13] we derived two variants of the Kramers-type formula in the presence of all diffusion coefficients D_{pp}, D_{qp}, and D_{qq}. These formulas were tested for $D_{qp}=0$ and $D_{qq}\neq 0$ to estimate the quasistationary probability rate through the barrier for a known potential and friction. In the case of $D_{qq}=0$ and $D_{qp}\neq 0$ the first variant of the formula is

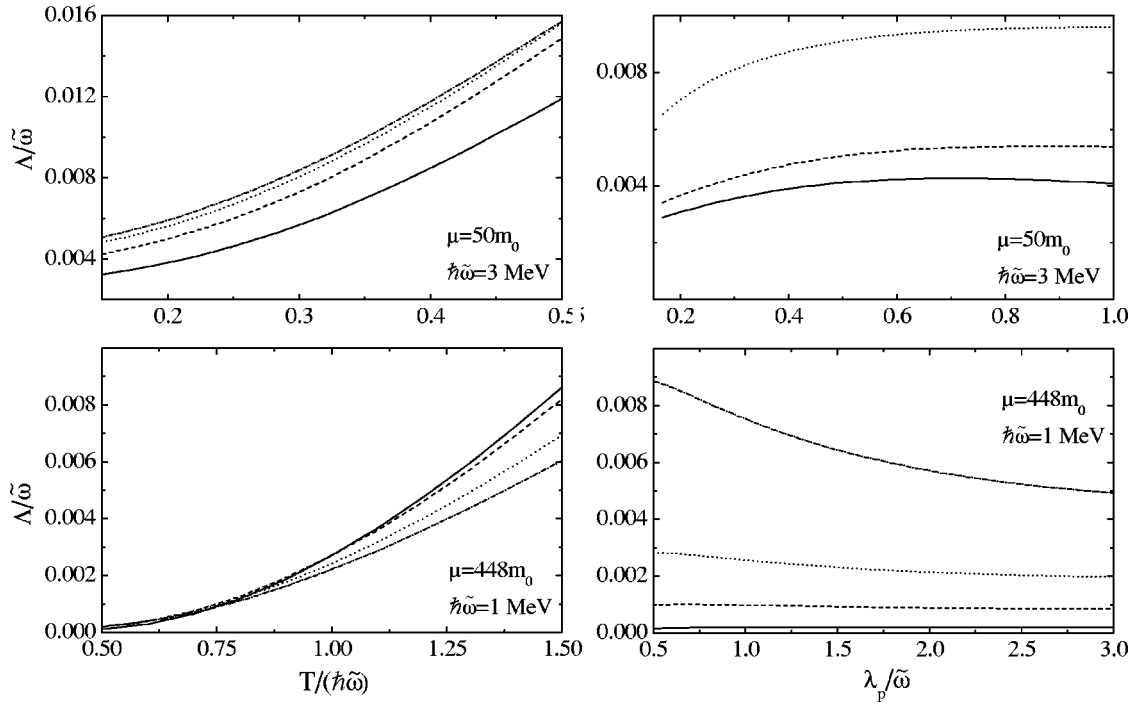

FIG. 9. Quasistationary value of the probability rate $\Lambda(t)/\tilde{\omega}$ from the left well in the potential (8) for $\mu=50m_0$ (upper part) and $\mu=448m_0$ (lower part) as a function of $T/(\hbar\tilde{\omega})$ and $\lambda_p/\tilde{\omega}$. The temperature dependence is presented for the friction coefficients $\lambda_p/\tilde{\omega}=0.5/(\hbar\tilde{\omega})$ (solid lines), $1.0/(\hbar\tilde{\omega})$ (dashed lines), $1.5/(\hbar\tilde{\omega})$ (dotted lines), and $2.0/(\hbar\tilde{\omega})$ (dash-dotted lines). The dependence on $\lambda_p/\tilde{\omega}$ is shown for the temperatures $T/(\hbar\tilde{\omega})=0.1/(\hbar\tilde{\omega})$ (solid line), $0.5/(\hbar\tilde{\omega})$ (dashed line), and $1.0/(\hbar\tilde{\omega})$ MeV (dotted line) in the upper part and $T/(\hbar\tilde{\omega})=0.5/(\hbar\tilde{\omega})$ (solid line), $0.75/(\hbar\tilde{\omega})$ (dashed line), $1.0/(\hbar\tilde{\omega})$ (dotted line), and $1.5/(\hbar\tilde{\omega})$ (dash-dotted line) in the lower part.

$$\Lambda = \frac{D_{pp}\tilde{\omega}}{2\pi\sqrt{D_{pp}(D_{pp}+2\mu\lambda_p D_{qp})}} \times \left(\frac{h}{\lambda_p - \frac{2\mu\lambda_p\omega_b^2 D_{qp}}{h(D_{pp}+2\mu\lambda_p D_{qp})} + h} \right)^{1/2} \times \exp\left[-\frac{V_L \mu\lambda_p}{D_{pp}+2\mu\lambda_p D_{qp}} \right], \quad (11)$$

where $h=-\lambda_p/2+(\lambda_p^2/4+\omega_b^2)^{1/2}$ and ω_b is the frequency of the inverted oscillator approximating the barrier. The second variant is a Kramers-type formula given by

$$\Lambda = \frac{\tilde{\omega}}{2\pi}\left(\frac{h}{\frac{D_{pp}}{\mu T^{eff}} - \frac{2\omega_b^2 D_{qp}(1-2D_{qp}/T^{eff})}{hT^{eff}} + h} \right)^{1/2} \times \exp\left[-\frac{V_L}{T^{eff}} \right], \quad (12)$$

where $T^{eff}=(D_{pp}+\mu\lambda_p D_{qp})/(\mu\lambda_p)$ and $h=\lambda_p/2-D_{pp}/(\mu T^{eff})+\{[\lambda_p/2-D_{pp}/(\mu T^{eff})]^2+\omega_b^2(1-4D_{qp}^2/T^{eff\,2})\}^{1/2}$. For $D_{qp}=0$, Eqs. (11) and (12) are simplified to the known Kramers formula [23] for the probability of escape over the potential barrier:

$$\Lambda^{Kr} = \frac{k\tilde{\omega}}{2\pi}\exp\left[-\frac{V_L}{\mu\tilde{\omega}^2\sigma_{qq}} \right], \quad (13)$$

where $k=[1+\lambda_p^2/(4\omega_b^2)]^{1/2}-\lambda_p/(2\omega_b)$.

For the potential (8), the quasistationary values Λ with respect to $\tilde{\omega}$ calculated from the solution of Eq. (2) with asymptotic values of the diffusion coefficients (5) are compared in Fig. 10 with the results obtained with Eqs. (11) and (12). Note that Eq. (11) holds good when the condition $\tilde{\omega}T/V_L<\lambda_p$ is valid [13]. This occurs for $\hbar\lambda_p>0.25T$ at $\hbar\omega=1$ MeV and for $\hbar\lambda_p>0.75T$ at $\hbar\tilde{\omega}=3$ MeV. For large $\tilde{\omega}$, the quantity $V_L-\hbar\tilde{\omega}/2$ is relatively small in the considered potential (8). Then the assumption of a long-living stationary state at the minimum of the potential becomes less justified. Therefore, in comparison to the treatment with a small frequency $\tilde{\omega}$, we find larger deviations of Λ between the analytical and numerical results (Fig. 10). However, for $\hbar\lambda_p$ between 1 and 2 MeV, the disagreement is only within a factor of 2 which is acceptable for many applications, especially in nuclear physics. The correspondence of numerical results obtained from the solution of Eq. (2) to the results following from the analytical expressions (11) and (12) demonstrates the validity of these expressions for the case of $D_{qp}\neq 0$.

IV. PURE STATES, UNCERTAINTY RELATION, AND DECOHERENCE

The linear entropy

$$D(t) = 1 - \mathrm{Tr}[\rho^2(t)] \quad (14)$$

can be considered as a measure of the purity of states. Since $\mathrm{Tr}[\rho^2(t)]\leqslant 1$, $D(t)$ is positive and equal to zero for a pure state. The purity of states decreases with increasing linear entropy. We can calculate the rate of entropy production from the master equation (2), assuming that the state remains approximately pure $\rho^2(t)\approx\rho(t)$:

$$\dot{D}(t) = -2\,\mathrm{Tr}[\rho(t)\dot{\rho}(t)] \approx \frac{4}{\hbar^2}[D_{qq}(t)\sigma_{pp}(t)+D_{pp}(t)\sigma_{qq}(t)-2D_{qp}(t)\sigma_{qp}(t)] - [\lambda_p(t)+\lambda_q(t)]. \quad (15)$$

If $\dot{D}(t)=0$ and $\mathrm{Tr}[\rho^2(0)]=1$, then $\mathrm{Tr}[\rho^2(t)]=1$ at all times $t>0$. This condition is necessary and sufficient to have $\rho^2(t)=\rho(t)$ all times. This means that $\rho(t)$ represents a pure state for $t\geqslant 0$. Under the special condition $\sigma(t)=\sigma_{pp}(t)\sigma_{qq}(t)-\sigma_{pq}^2(t)=\hbar^2/4$, the set of diffusion coefficients,

$$D_{qq}(t) = \frac{1}{2}[\lambda_p(t)+\lambda_q(t)]\sigma_{qq}(t),$$

$$D_{pp}(t) = \frac{1}{2}[\lambda_p(t)+\lambda_q(t)]\sigma_{pp}(t),$$

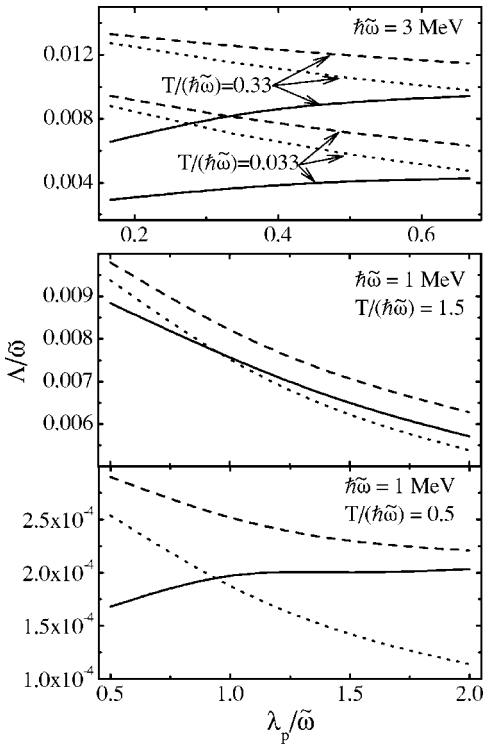

FIG. 10. Quasistationary decay rate $\Lambda/\tilde{\omega}$ through the barriers in the potential presented in Fig. 2 for $\mu=50m_0$ ($\hbar\tilde{\omega}=3$ MeV) and $\mu=448m_0$ ($\hbar\tilde{\omega}=1$ MeV) as a function of $\lambda_p/\tilde{\omega}$ with the initial Gaussian packet at the left-hand minimum for the indicated temperatures $T/(\hbar\tilde{\omega})$. The numerically calculated results obtained from Eq. (10) by solving Eq. (2) with the set (4) of diffusion coefficients are presented by solid lines. The results obtained with Eqs. (11) and (12) are presented by the dashed and dotted lines, respectively.

$$D_{qp}(t) = \frac{1}{2}[\lambda_p(t) + \lambda_q(t)]\sigma_{qp}(t), \tag{16}$$

satisfies the pure state condition $\dot{D}(t)=0$, at which the pure states remain pure for all times. With Eqs. (16) the condition (3) is fulfilled. If the variances of the pure state are assumed to be constant $\sigma_{ij}(t)=\sigma_{ij}(0)=\sigma_{ij}(\infty)$ $(i,j=q,p)$ and hold the minimum uncertainty equality $\sigma(t)=\hbar^2/4$, then we obtain the following diffusion coefficients for pure states in the case of a harmonic oscillator from Eqs. (27)–(29) of paper I [1]:

$$D_{qq}(t) = \lambda_q(t)\sigma_{qq}(0) - \frac{1}{m(t)}\sigma_{qp}(0),$$

$$D_{pp}(t) = \lambda_p(t)\sigma_{pp}(0) + \xi(t)\sigma_{qp}(0),$$

$$D_{qp}(t) = \frac{1}{2}\left([\lambda_p(t) + \lambda_q(t)]\sigma_{qp}(0) + \xi(t)\sigma_{qq}(0) - \frac{1}{m(t)}\sigma_{pp}(0)\right). \tag{17}$$

Using Eqs. (17), we can show that the equality $\dot{D}(t)=0$ is fulfilled at any time for the pure states. To form the pure state, the random and dissipative forces must satisfy the following equations [see Eq. (14) of [1]]:

$$J_{q_tq_t} = (1 - A_t^2)\sigma_{qq}(0) - B_t^2\sigma_{pp}(0) - 2A_tB_t\sigma_{qp}(0),$$

$$J_{p_tp_t} = (1 - N_t^2)\sigma_{pp}(0) - M_t^2\sigma_{qq}(0) - 2N_tM_t\sigma_{qp}(0),$$

$$\frac{1}{2}(J_{q_tp_t} + J_{p_tq_t}) = (1 - A_tN_t - B_tM_t)\sigma_{qp}(0) - A_tM_t\sigma_{qq}(0) - B_tN_t\sigma_{pp}(0). \tag{18}$$

The explanations of all notations in Eqs. (17) and (18) are given in Ref. [1]. For the particular case of a pure state of the FC oscillator ($\lambda_q=\sigma_{qp}=0$), we obtain, from Eqs. (17),

$$D_{qq}(t) = 0,$$

$$D_{pp}(t) = \lambda_p(t)\sigma_{pp}(0),$$

$$D_{qp}(t) = \frac{1}{2}\left[\xi(t)\sigma_{qq}(0) - \frac{1}{\mu}\sigma_{pp}(0)\right], \tag{19}$$

where $\xi(\infty)=\mu\tilde{\omega}^2$. This set of diffusion coefficients was also derived in Ref. [24] in a completely different way but the assurance of the purity of states with them was not mentioned.

The equation for $\dot{\sigma}(t)$ in the case of a harmonic oscillator follows from Eqs. (26) of [1]:

$$\dot{\sigma}(t) = -2[\lambda_p(t) + \lambda_q(t)]\sigma(t) + 2[D_{pp}(t)\sigma_{qq}(t) + D_{qq}(t)\sigma_{pp}(t) - 2D_{qp}(t)\sigma_{qp}(t)]. \tag{20}$$

If the state remains approximately pure $[\rho^2(t)\approx\rho(t)]$, then, from Eqs. (15) and (20),

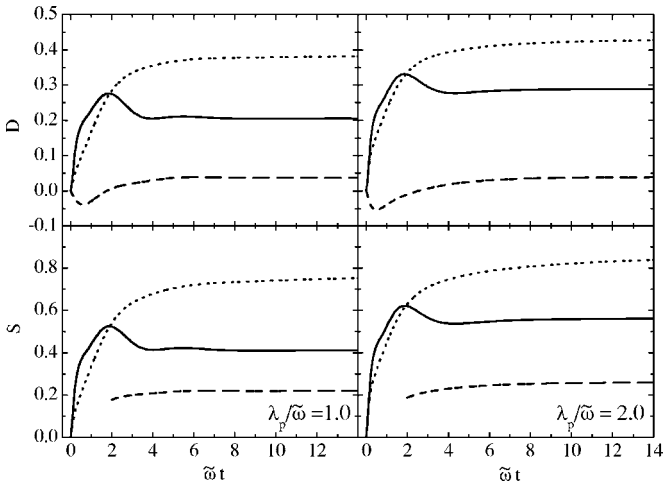

FIG. 11. Time dependence of the linear entropy $D(t)$ (upper part) and of the von Neumann entropy $S(t)$ (lower part) for the wave packet initially being in the left-hand well of the potential presented in Fig. 2 for $\mu=448m_0$ ($\hbar\tilde{\omega}=1$ MeV), $T/(\hbar\tilde{\omega})=0.1$, and the indicated values of $\lambda_p/\tilde{\omega}$. The results obtained with the diffusion coefficients (4), (6), and (7) are shown by solid, dotted, and dashed lines, respectively.

$$\dot{\sigma}(t) \approx -2[\lambda_p(t) + \lambda_q(t)]\left[\sigma(t) - \frac{\hbar^2}{4}\right] + \frac{\hbar^2}{2}\dot{D}(t).$$

One can see that the rate of $\sigma(t)$ is explicitly connected with the rate of entropy production. An important consequence of Eq. (20) is the fact that $\sigma\geqslant\hbar^2/4$ is fulfilled for any state (pure or mixture) if $\sigma(0)\geqslant\hbar^2/4$:

$$D_{pp}(t)\sigma_{qq}(t) + D_{qq}(t)\sigma_{pp}(t) - 2D_{qp}(t)\sigma_{qp}(t) \geqslant \frac{\hbar^2}{4}[\lambda_p(t) + \lambda_q(t)]. \tag{21}$$

For $t\to\infty$ we have, from Eqs. (20),

$$D_{pp}(\infty)\sigma_{qq}(\infty) + D_{qq}(\infty)\sigma_{pp}(\infty) - 2D_{qp}(\infty)\sigma_{qp}(\infty) = \sigma(\infty)[\lambda_p(\infty) + \lambda_q(\infty)]. \tag{22}$$

The relation (21) is the generalization of the inequality for Markovian dynamics to the case of non-Markovian dynamics.

The problem of entropy production has been addressed in Refs. [25–30]. Figure 11 shows the linear entropy for the potential (8) and diffusion coefficients (4). It starts from zero because we set a nearly pure state in the left well as the initial condition for the solution of Eq. (2) and it has a positive value for all time of the evolution. In the case of the classic diffusion coefficients (7), $D(t)$ can be negative during a short initial time interval that correlates with the negativity of $u(t)$ in Fig. 5. The linear entropy (decoherence) has larger values for larger T and λ_p. Since the potential (8) is not the harmonic oscillator, $D(t)$ can oscillate and is always positive with diffusion coefficients (4). The time behavior of the nondiagonal components of the density matrix is correlated with the time dependence of the linear entropy.

We also calculate the von Neumann entropy

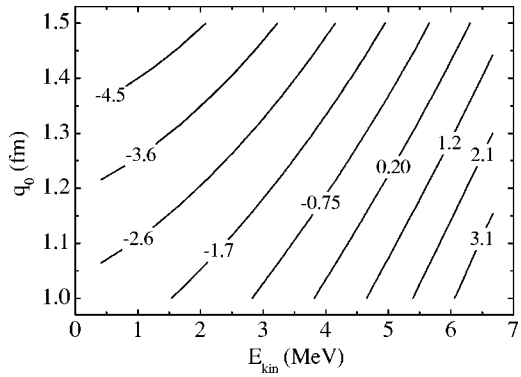

FIG. 12. Dependence of the average initial total energy E_0 in MeV of the Gaussian packet on its position q_0 and kinetic energy E_{kin} in the potential shown in Fig. 2.

$$S(t) = -\mathrm{Tr}\{\rho(t)\ln[\rho(t)]\}.$$

One can see from Fig. 11 that the time dependences of $S(t)$ and $D(t)$ are almost the same. After the initial exponential increases the entropy becomes linear in t at $0.5 \leqslant \tilde{\omega}t \leqslant 2$. At larger time, $\tilde{\omega}t > 4$, the quasistationary regime is settled in the example considered and $S(t)$ $[D(t)]$ increases very slowly. This increase with small rate contains the Kolmogorov-Sinai regime [25–30]. Since in the considered example only small fraction (less than 1%) of the system wave function is in the region of barrier where the Lyapunov exponent is positive, the Kolmogorov-Sinai regime is not pronounced. In a forthcoming publication we will treat the inverted oscillator for which the rate of von Neumann entropy coincides with the Kolmogorov-Sinai entropy after the system becomes Markovian. For the inverted oscillator, the Kolmogorov-Sinai regime is expected to be very pronounced.

V. CAPTURE PROBABILITY

Let us study the capture of an initially Gaussian packet moving towards the barrier at $q=0$ from the right-hand side with some kinetic energy into the left-hand well (see Fig. 2). The capture probability $P_c(t)$ is defined in analogy to the probability of the penetrability in Eq. (9):

$$P_c(t) = \int_{-\infty}^{q_b} dq[\rho(q,t) - \rho(q,t=0)] \Big/ \int_{q_b}^{\infty} dq\, \rho(q,0). \tag{23}$$

When the packet approaches the barrier, the value of $P_c(t)$ increases up to the quasistationary value P_c which defines the part of the initial packet captured in the left-hand well. Due to the friction, the value of P_c depends on the initial position q_0 of the packet as well as on the initial kinetic energy $E_{kin}=p_0^2/(2\mu)$. The dependence of the average initial total energy $E_0=\mathrm{Tr}(\hat{\rho}H_0)$ of the Gaussian packet with $\sqrt{\sigma_{qq}(0)}=0.35$ fm and $\sigma_{pp}(0)=\hbar^2/[4\sigma_{qq}(0)]$ is presented as function of q_0 and E_{kin} in Fig. 12 for the potential (8). The capture probabilities $P_c(t)$ are presented for various q_0 and E_{kin} in Fig. 13. The asymptotic values $P_c(\infty)$ on λ_p are shown

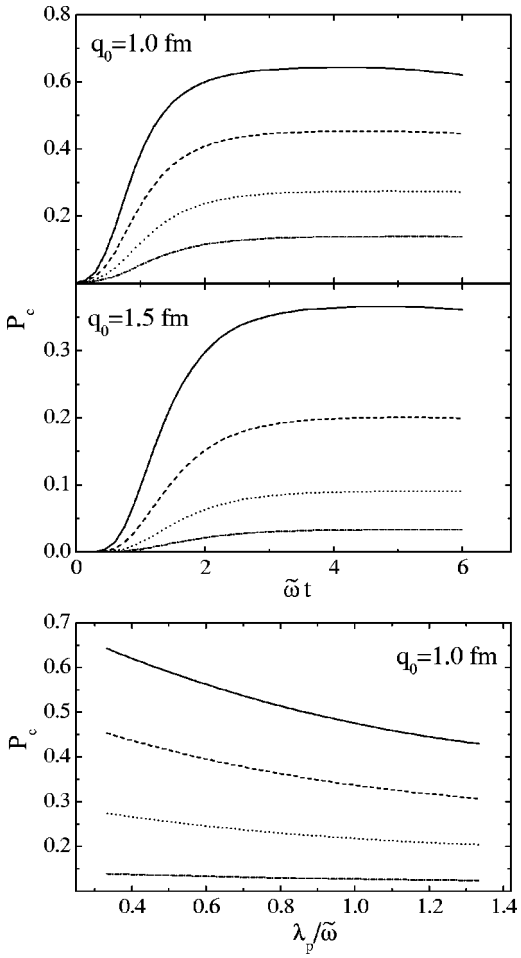

FIG. 13. The capture probability of the Gaussian packet into the left-hand well of the potential (8) as a function of time (upper two figures) at $q_0=1$ and 1.5 fm for $\mu=50m_0$ and $\lambda_p/\tilde{\omega}=0.33$. The dependence of the asymptotic capture probability on $\lambda_p/\tilde{\omega}$ shown in the lowest figure. The results for $E_{kin}=6.7$, 3.8, 1.8, and 0.4 MeV are presented by solid, dotted, dashed, and dot-dashed lines, respectively.

as well. One can see that even for energies exceeding the barrier only a part of the packet is captured and, therefore, $P_c<1$. For the energies near the barrier, the dependence of $P_c(\infty)$ on λ_p is rather weak. For the energies well above the barrier, the friction suppresses the capture stronger. Therefore, the present results can be useful for calculating capture cross sections in the nucleus-nucleus collisions where the capture occurs into a shallow well of the potential.

VI. SUMMARY

With the exact numerical solution of Eq. (2) for the reduced density matrix we found a minor role of the time dependence of the friction and diffusion coefficients in the escape rate from a potential well. Since the used friction and diffusion coefficients were self-consistently under certain approximations derived, they preserve the positivity of the density matrix at any time. The diffusion coefficient D_{qp} leads to a decrease of the escape rate. Since the used value of D_{pp} is

larger than the one following from a classic treatment, the obtained escape rate is close to the rate calculated with the classic set of diffusion coefficients. If the regime of motion is close to the underdamped case or the temperature is small, the quasistationary escape rate can increase with friction. This is explained by the larger role of the increasing diffusion in the decay process. The agreement of the escape rate obtained with the analytical expressions in comparison to numerically calculated data depends on the characteristics of the considered system. The agreement is better in the overdamped regime. However, for any regime the deviations are not larger than in the case of the classical Kramers formula. Therefore, the analytical expressions can be applied in a large range of parameters for the potential and diffusion coefficients. We demonstrated that the uncertainty function $\sigma(t)$ is related to the linear entropy. The diffusion coefficients supplying the purity of states were elaborated for the non-Markovian dynamics. The obtained dependences of the capture probability on the friction proves that the quantum nature of this process should be taken into consideration when one calculates the capture cross section in nucleus-nucleus collisions.

ACKNOWLEDGMENTS

This work was supported in part by Volkswagen-Stiftung (Hannover), DFG (Bonn), RFBR (Moscow), and STCU (Tashkent).

[1] Z. Kanokov, Yu. V. Palchikov, G. G. Adamian, N. V. Antonenko, and W. Scheid, preceding paper, Phys. Rev. E **71**, 016121 (2005).
[2] E. G. Harris, Phys. Rev. A **48**, 995 (1993).
[3] K. Fujikawa, S. Iso, M. Sasaki, and H. Suzuki, Phys. Rev. Lett. **68**, 1093 (1992).
[4] U. Weiss, *Quantum Dissipative Systems* (World Scientific, Singapore, 1992).
[5] S. Baskoutas and A. Jannussis, J. Phys. A **25**, L1299 (1992).
[6] G. W. Ford, J. T. Lewis, and R. F. O'Connel, Phys. Lett. A **158**, 367 (1991).
[7] M. Razavy and A. Pimpale, Phys. Rep. **168**, 305 (1988); M. Razavy, Phys. Rev. A **41**, 6668 (1990).
[8] A. O. Caldeira and A. J. Leggett, Phys. Rev. Lett. **46**, 211 (1981); **48**, 1571 (1982); Ann. Phys. (N.Y.) **149**, 374 (1983).
[9] A. Widom and T. D. Clark, Phys. Rev. Lett. **48**, 63 (1982); Phys. Rev. B **30**, 1205 (1984).
[10] R. Bruinsma and Per Bak, Phys. Rev. Lett. **56**, 420 (1986).
[11] G. G. Adamian, N. V. Antonenko, and W. Scheid, Phys. Lett. A **244**, 482 (1998); **260**, 39 (1999).
[12] Yu. V. Palchikov, G. G. Adamian, N. V. Antonenko, and W. Scheid, J. Phys. A **33**, 4265 (2000).
[13] Yu. V. Palchikov, G. G. Adamian, N. V. Antonenko, and W. Scheid, Physica A **316**, 297 (2002).
[14] W. T. Strunz, J. Phys. A **30**, 4053 (1997).
[15] A. A. Belavin, B. Ya. Zel'dovich, A. M. Perelomov, and B. S. Popov, Sov. Phys. JETP **56**, 264 (1969).
[16] E. B. Davies, *Quantum Theory of Open Systems* (Academic, New York, 1976).
[17] G. Lindblad, Commun. Math. Phys. **48**, 119 (1976); Rep. Math. Phys. **10**, 393 (1976).
[18] H. Dekker, Phys. Rep. **80**, 1 (1981).
[19] V. V. Dodonov and V. I. Man'ko, Rep. Phys. Inst. **167**, 7 (1986).
[20] A. Sandulescu and H. Scutaru, Ann. Phys. (N.Y.) **173**, 277 (1987).
[21] A. Isar, A. Sandulescu, H. Scutaru, E. Stefanescu, and W. Scheid, Int. J. Mod. Phys. A **3**, 635 (1994).
[22] H. Hofmann and D. Kiderlen, Int. J. Mod. Phys. A **7**, 243 (1998).
[23] H. A. Kramers, Physica (Amsterdam) **7**, 284 (1940).
[24] R. Karrlein and H. Grabert, Phys. Rev. E **55**, 153 (1997).
[25] A. Isar, Fortschr. Phys. **47**, 855 (1999).
[26] V. Latora and M. Baranger, Phys. Rev. Lett. **82**, 520 (1999).
[27] A. K. Pattanayak, Phys. Rev. Lett. **83**, 4526 (1999).
[28] P. Grigolini, M. G. Pala, L. Palatella, and R. Roncaglia, Phys. Rev. E **62**, 3429 (2000).
[29] M. Bologna, P. Grigolini, M. Karagiorgis, and A. Rosa, Phys. Rev. E **64**, 016223 (2001).
[30] P. Grigolini, M. G. Pala, and L. Palatella, Phys. Lett. A **285**, 49 (2001).